Coordination Chemistry Reviews 254 (2010) 2472–2482

Contents lists available at ScienceDirect

Coordination Chemistry Reviews

journal homepage: www.elsevier.com/locate/ccr

Review

Toward more efficient photochemical CO_2 reduction: Use of $scCO_2$ or photogenerated hydrides

Mark D. Doherty, David C. Grills, James T. Muckerman, Dmitry E. Polyansky, Etsuko Fujita*

Chemistry Department, Brookhaven National Laboratory, Upton, NY 11973-5000, USA

Contents

ARTICLE INFO

Article history:
Received 25 September 2009
Accepted 6 December 2009
Available online 8 January 2010

Keywords:
Carbon dioxide reduction
Small molecule activation
Photocatalysis
Renewable hydride donors
Supercritical CO_2
NADH-model ligands

ABSTRACT

Rhenium(I) and ruthenium(II) complexes have been successfully used for photochemical CO_2 reduction to CO or formate. However, a typical turnover frequency for such reactions is <20 h^{-1} and the formation of reduced species beyond CO or formate is very limited. In the case of the rhenium(I) bipyridyl tricarbonyl system, the key intermediate has been shown to decay with a first-order dependence on [CO_2] to produce CO, which is the rate-determining step. The limited concentration of dissolved CO_2 in organic solvents results in extremely slow CO_2 reduction. To improve the reaction rate, we prepared new CO_2-soluble rhenium(I) bipyridine complexes bearing fluorinated alkyl ligands and investigated their photophysical properties in CH_3CN and supercritical CO_2. We also investigated the properties of a metal complex with an NAD^+ model ligand, $[Ru(bpy)_2(pbn)]^{2+}$ (bpy = 2,2′-bipyridine, pbn = 2-(2-pyridyl)-benzo[*b*]-1,5-naphthyridine), and prepared the corresponding NADH-like complex $[Ru(bpy)_2(pbnHH)]^{2+}$ upon MLCT excitation followed by reductive quenching. This species can be used as a renewable hydride donor. The electrochemical and photochemical properties, and the reactivity of these species toward CO_2 reduction were investigated.

1. Introduction

There is currently a considerable research effort into the development of efficient methods for Carbon Capture and Storage (CCS), in which CO_2 from industrial and energy-related sources would be captured and stored indefinitely. This has been prompted by rapidly rising atmospheric CO_2 levels (currently at ~386 ppm [1]), which threaten to cause catastrophic environmental damage through global warming [2–4]. However, an attractive alternative to storing the captured CO_2 would be to make use of it as a feedstock for the production of clean fuels, such as methanol and methane, and/or fine chemicals. Being the final product of combustion, CO_2 is a thermodynamically stable and inert molecule. Thus, its conversion into higher-energy reduced forms requires the input of large amounts of energy and catalysts to mediate the reactions. Therefore, if such a process is to become economically viable, a renewable source of energy is essential. One of the most promising strategies would be to make use of solar energy in so-called 'artificial photosynthetic' processes, in which simple chemical transformations, inspired by the more complex natural photosystems, convert CO_2 into reduced forms. This type of photochemical CO_2 reduction has been the subject of intense research for a number of years now. As can be seen in Table 1, the electrochemical potential for the direct one-electron reduction of CO_2 to $CO_2^{\bullet-}$ is −1.90 V vs. NHE, making this a highly unfavorable process [5]. Large kinetic overpotentials are also observed for this electrochemical reduction due to the barrier arising from the conversion of linear CO_2 into bent $CO_2^{\bullet-}$. In contrast, proton-assisted multielectron processes, although often kinetically challenging, are much more thermodynamically favorable (see Table 1) [6]. Though stoichiometric conversions of CO_2 have been reported, many of which are currently used in industry, this paper will focus on photocatalytic reactions using transition-metal complexes as catalysts.

* Corresponding author at: Chemistry Department, Brookhaven National Laboratory, Bldg 555, Upton, NY 11973-5000, USA. Tel.: +1 631 344 4356.
E-mail address: fujita@bnl.gov (E. Fujita).

0010-8545/$ – see front matter © 2010 Elsevier B.V. All rights reserved.
doi:10.1016/j.ccr.2009.12.013

Table 1
Reduction potentials for various CO_2 reduction reactions in aqueous solution at pH 7 vs. NHE. All other solutes at 1 M.

Reaction	$E^{0'}$ (V)
$CO_2 + e^- \rightarrow CO_2^{\bullet -}$	−1.90
$CO_2 + H^+ + 2e^- \rightarrow HCO_2^-$	−0.49
$CO_2 + 2H^+ + 2e^- \rightarrow HCO_2H$	−0.61
$CO_2 + 2H^+ + 2e^- \rightarrow CO + H_2O$	−0.53
$CO_2 + 4H^+ + 4e^- \rightarrow C + 2H_2O$	−0.20
$CO_2 + 4H^+ + 4e^- \rightarrow HCHO + H_2O$	−0.48
$CO_2 + 6H^+ + 6e^- \rightarrow CH_3OH + H_2O$	−0.38
$CO_2 + 8H^+ + 8e^- \rightarrow CH_4 + 2H_2O$	−0.24

The use of metal-based catalysts has several advantages. For example, through careful ligand and metal modifications, the absorption spectrum of the catalyst can be tuned to capture visible light within the solar spectrum. Furthermore, upon absorption of light these complexes often exhibit long-lived charge-separated excited states that can be efficiently coupled with multielectron-redox processes to activate and reduce CO_2. Thus, the use of such catalysts avoids high-energy intermediates and facilitates the coupling of electron transfer to bond-forming reactions, generally through an initial coordination of a CO_2 molecule to a vacant coordination site of the reduced form of the catalyst. The metal complexes may act as photosensitizers, working in combination with secondary electron relay catalysts to couple the photon energy to the chemical reduction, or they may be catalysts that are sensitized by organic or inorganic photosensitizers, or they can combine both functions into a single species.

Researchers in this field have achieved the efficient coupling of light absorption and charge separation with dark catalytic reactions to produce CO and formate under a variety of conditions (Table 2) [4,6]. The photocatalytic CO_2 reduction systems listed in Table 2 can be grouped into four general categories: (1) $Ru(bpy)_3^{2+}$ type complexes as a photosensitizer with a metal colloid or metal complex (including $Ru(bpy)_3^{2+}$) as a catalyst; (2) organic photosensitizers with a metal complex as a catalyst; (3) metal porphyrin complexes as both a photosensitizer and a catalyst; and (4) *fac*-$ReX(bpy)(CO)_3$ type complexes as both a photosensitizer and a catalyst. We are especially interested in catalyst systems belonging to group (4) which have recently been reported to be capable of achieving quantum yields for CO formation of 59% using a dual $Re(bipyridyl)(CO)_3X$-type photosensitizer-catalyst system [7]. However, typical turnover frequencies and turnover numbers for CO formation are less than 20 h^{-1} and ~250, respectively, owing to the nature of the extremely stable CO_2 molecule and low stability of catalysts and/or photosensitizers. There exist even more formidable challenges for CO_2 utilization. For example, in order to use the current infrastructure, a liquid fuel, e.g., methanol, has to be photochemically produced from CO_2. Furthermore, we need to couple reductive (*i.e.*, CO_2 reduction) and oxidative (*i.e.*, water oxidation) half-reactions to eliminate the use of a sacrificial electron donor. In this review, we will discuss molecular approaches toward: (1) more efficient photochemical reduction of CO_2 using CO_2-soluble tricarbonyl rhenium complexes with bpy-type ligands in supercritical CO_2 and (2) CO_2 reduction beyond CO using photogenerated renewable hydride donors.

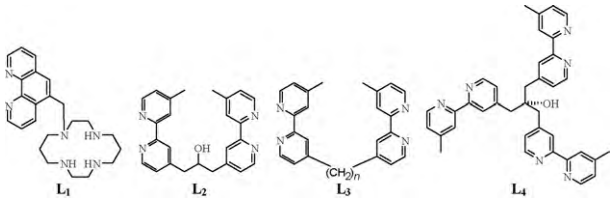

Chart 1. Structures of ligands $\mathbf{L_1}$–$\mathbf{L_4}$.

2. Photochemical CO_2 reduction using tricarbonyl rhenium(I) complexes with 2,2′-bipyridine (bpy) or similar ligands

Complexes of the general formula *fac*-$ReX(\alpha\text{-diimine})(CO)_3^n$ (α-diimine = bpy or substituted bpy and $n = 0$, $X = Cl^-$, Br^-; $n = +1$, $X = PR_3$, solvent, etc.) have been shown to effectively catalyze the reduction of CO_2 to CO in the presence of sacrificial electron donors, under the appropriate photochemical conditions. These complexes typically possess intense metal-to-ligand charge transfer (MLCT) absorption bands between 340 and 500 nm depending on the ligand set and solvent [43,44]. Initial light absorption produces a ^{3}MLCT excited state, which is emissive in solution with excited state lifetimes ranging from 27 ns ($X = Cl^-$, α-diimine = bpy) [45] to 1034 ns ($X = P(OEt)_3$, α-diimine = bpy) [46] in CH_3CN. Quantum yields for CO formation using these complexes have been reported, ranging from $\Phi_{CO} = 0.14$ ($X = Cl^-$, α-diimine = bpy) [27,28,43] to $\Phi_{CO} = 0.38$ ($X = P(OEt)_3$, α-diimine = bpy) [33], with the highest value of $\Phi_{CO} = 0.59$ reported for a dual component photosensitizer-catalyst system consisting of a 25:1 ratio of [*fac*-(4,4′-$(MeO)_2$-bpy)$(CO)_3$Re{$P(OEt)_3$}][PF_6]:[*fac*-(bpy)$(CO)_3$Re(CH_3CN)][PF_6] [7].

Mechanistic studies of electrocatalytic CO_2 reduction with these rhenium complexes have led to the proposal of simultaneous one- and two-electron pathways leading to CO formation with a current efficiency of 98% [47,48]. Using *fac*-ReCl(bpy)$(CO)_3$ as an example, the first step involves the generation of a one-electron reduced (OER) species [*fac*-ReCl(bpy)$(CO)_3$]$^-$ (see Fig. 1) at −1.5 V vs. SCE in CO_2-saturated CH_3CN [48]. Loss of Cl^- from this OER species is slow, producing a 17e$^-$ metal-centered radical [*i.e.*, *fac*-$Re^{\bullet}$(bpy)$(CO)_3$], which in polar solvents (CH_3CN, THF, DMF, etc.) is rapidly trapped by a solvent molecule to form the ligand-centered radical, [*fac*-Re^{I}(bpy$^{\bullet -}$)$(CO)_3$(solv)]. In the one-electron pathway [47,48], it is proposed that solvent is replaced by CO_2 and subsequent reductive disproportionation with another CO_2 molecule forms CO and CO_3^{2-}. For the two-electron pathway [47] reduction of the solvent-coordinated radical at −1.8 V vs. SCE in CH_3CN results in the formation of a five coordinate 18e$^-$ metal-based anion, [*fac*-Re(bpy)$(CO)_3$]$^-$. Subsequent coordination of CO_2 followed by reaction with additional CO_2 as an oxide acceptor (Fig. 1) produces CO and CO_3^{2-}. After CO formation, both one- and two-electron pathways form a cationic solvent-coordinated species, [*fac*-Re(bpy)$(CO)_3$(solv)]$^+$ which upon reduction regenerates the solvent-coordinated ligand-centered radical species, closing the catalytic cycle. While the OER and [*fac*-Re(bpy)$(CO)_3$]$^-$ have been observed using infrared spectroelectrochemical techniques [47], neither of the proposed CO_2 adducts, [*fac*-Re(bpy)$(CO)_3(CO_2)$]$^{\bullet}$ or [*fac*-Re(bpy)$(CO)_3(CO_2)$]$^-$ have been observed during catalysis. Very little is known about the C=O bond cleavage steps involved in CO formation by the one- or two-electron pathways, however several species including metallocarboxylate and metallocarboxylic acid complexes have been postulated as intermediates [47–49].

Similar one- and two-electron mechanistic pathways have been proposed for the photochemical reduction of CO_2 using these rhenium catalysts based on a number of reactions which have been observed spectroscopically. Initial photoexcitation of *fac*-ReCl(dmb)$(CO)_3$ (dmb = 4,4′-dimethyl-2,2′-bipyridine) followed by reductive quenching by a tertiary amine (NEt_3 (TEA) or $N(CH_2CH_2OH)_3$ (TEOA)) produces an analogous OER species (*vide supra*) [50]. Rapid solvation following chloride

Table 2
Some examples of photochemical CO_2 reduction systems, products, catalytic activities and quantum yields.[a].

Sensitizer	Catalyst or relay	Donor	Product (s)	Φ[b] (mol einstein^{-1})	TON/TOF[c]	Ref.
$Ru(bpy)_3^{2+}$		TEOA	$HCOO^-$	0.049[d]	19/9.5	[8]
$Ru(bpy)_3^{2+}$		TEOA	$HCOO^-$	0.096[e]	43/21.5	[8]
$Ru(bpy)_3^{2+}$	MV^{2+}	TEOA	$HCOO^-$	0.01	75/18.8	[9]
$Ru(bpy)_3^{2+}$	Co^{2+}/bpy	TPA	CO, H_2		9/0.4	[10]
$Ru(bpy)_3^{2+}$	Co^{2+}/Me_2phen	TEA	CO, H_2	0.012 (CO), 0.065 (H_2)		[11]
$Ru(bpy)_3^{2+}$	$Ru(bpy)_2(CO)_2^{2+}$	TEOA	$HCOO^-$	0.14		[12–14]
$Ru(bpy)_3^{2+}$	$Ru(bpy)_2(CO)_2^{2+}$	BNAH	$HCOO^-$, CO	0.03 ($HCOO^-$), 0.15 (CO)		[12–14]
$Ru(bpy)_3^{2+}$	$Ru(bpy)_2(CO)H^+$	TEOA	$HCOO^-$	0.15	161/80.5	[8]
$Ru(bpy)_3^{2+}$	$Ru(bpy)_2(CO)(X)^{n+}$ X = Cl, CO	TEOA	$HCOO^-$		163/81.5 (X = Cl) 54/27 (X = CO)	[8]
$Ru(bpy)_3^{2+}$	$Co(HMD)^{2+}$	H_2A	CO, H_2			[15]
$Ru(bpy)_3^{2+}$	$Ni(cyclam)^{2+}$	H_2A	CO, H_2	0.001 (CO)		[16,17]
$Ru(phen)_3^{2+}$	$Ni(cyclam)^{2+}$	H_2A	CO, H_2		<0.1	[18]
$[(phen)_2Ru(L_1)Ni]^{2+}$		H_2A	CO, H_2		<0.1	[18]
$Ru(bpy)_3^{2+}$	$Ni(Pr\text{-}cyclam)^{2+}$	H_2A	CO, H_2	ca. 0.005 (CO)		[19]
$Ru(bpz)_3^{2+}$	Ru colloid	TEOA	CH_4	10^{-4} (CH_4)[f]		[20,21]
$Ru(bpy)_3^{2+}$	bipyridinium$^+$, Ru or Os colloid	TEOA	CH_4, H_2	10^{-4} (CH_4)[f], 10^{-3} (H_2)[f]		[21]
p-Terphenyl	$Co(cyclam)^{3+}$	TEOA	CO, $HCOO^-$, H_2	0.25 ($CO + HCOO^-$)[f]		[22]
p-Terphenyl	$Co(HMD)^{2+}$	TEOA	CO, $HCOO^-$, H_2			[22,23]
Phenazine	$Co(cyclam)^{3+}$	TEOA	$HCOO^-$	0.07[f]		[24]
$Fe^{III}(TPP)$		TEA	CO		70/23	[25]
$Co^{III}(TPP)$		TEA	$HCOO^-$, CO		>300/100 ($HCOO^- + CO$)	[26]
$ReCl(bpy)(CO)_3$		TEOA	CO	0.14[g]	23/11.5	[27,28]
$ReCl(bpy)(CO)_3$		TEA	CO		42/1.7[h]	[29]
$ReBr(bpy)(CO)_3$		TEOA	CO	0.15[i]	21/10.5	[27,30,31]
$Re(OCHO)(bpy)(CO)_3$		TEOA	CO	0.05	12/3	[28,32]
$[Re(bpy)(CO)_3(PR_3)]^+$		TEOA	CO	0.38 (R = OEt), 0.013 (R = *n*Bu), 0.024 (R = Et), 0.2 (R = O*i*Pr), 0.17 (R = OMe)	7.5/0.5 (R = OEt), <1/<0.1 (R = *n*Bu, Et), 6.2/0.5 (R = O*i*Pr), 5.5/0.4 (R = OMe)	[33,34]
$[Re(4,4'\text{-}(MeO)_2\text{-}bpy)(CO)_3\{P(OEt)_3\}]^+$	$[Re(bpy)(CO)_3(CH_3CN)]^+$	TEOA	CO	0.59		[7]
$[Re(bpy)(CO)_3\{P(Ohex)_3\}]^+$		TEA	CO		2.2/1.1[j]	[35]
$[Re(bpy)(CO)_3\{P(O\textit{i}Pr)_3\}]^+$		TEOA	CO		15.6/0.7[h]	[36]
$[Re(dmb)(CO)_3\{P(OEt)_3\}]^+$		TEOA	CO	0.18	4.1/0.2	[34]
$[Re(4,4'\text{-}(CF_3)_2\text{-}bpy)(CO)_3\{P(OEt)_3\}]^+$		TEOA	CO	0.005	<1, <0.1	[34]
$[Re(bpy)(CO)_3(4\text{-}X\text{-}py)]^+$		TEOA	CO	0.03 (X = *t*Bu, Me, H), 0.04 (X = C(O)Me), 0.13 (X = CN)	1/0.1 (X = *t*Bu, H, Me, C(O)Me), 3.5/0.4 (X = CN)	[37]
$Ru(dmb)_3^{2+}$	$ReCl(dmb)(CO)_3$	BNAH	CO	0.062	101/6.3	[38]
$[(dmb)_2Ru(L_2)Re(CO)_3Cl]^{2+}$		BNAH	CO	0.12	170/10.7	[38]
$[(dmb)_2Ru(L_2)Re(CO)_3\{P(OEt)_3\}]^{3+}$		BNAH	CO	0.21	232/19.3	[39]
$[Ru\{(L_2)Re(CO)_3Cl\}_3]^{2+}$		BNAH	CO	0.093	240/15	[38]
$[(dmb)_2Ru(L_3)Re(CO)_3Cl]^{2+}$		BNAH	CO	0.13 (*n* = 2), 0.11 (*n* = 4, 6)	180/15 (*n* = 2), 120/10 (*n* = 4, 6)	[40]
$[(dmb)_2Ru(L_4)\{Re(CO)_3Cl\}_2]^{2+}$		BNAH	CO		190/11.8	[41,42]
$[\{(dmb)_2Ru\}_2(L_4)Re(CO)_3Cl]^{4+}$		BNAH	CO		110/6.9	[41,42]

[a] Abbreviations used: TEOA, triethanolamine; MV^{2+}, methylviologen; TPA, tripropylamine; TEA, triethylamine; bpy, 2,2′-bipyridine; dmb, 4,4′-dimethyl-2,2′-bipyridine; bpz, 2,2′-bipyrazine; phen, 1,10-phenanthroline; Me_2phen, 2,9-dimethyl-1,10-phenanthroline; BNAH, 1-benzyl-1,4-dihydronicotinamide; H_2A, ascorbic acid; HMD, 5,7,7,12,14,14-hexamethyl-1,4,8,11-tetraazacyclotetradeca-4,11-diene; cyclam, 1,4,8,11-tetraazacyclotetradecane; Pr-cyclam, 6-((N-R)pyridin-4-yl)methyl-1,4,8,11-tetraazacyclotetradecane where R, *p*-methoxybenzyl and benzyl; TPP, 5,10,15,20-tetraphenyl-21H,23H-porphine. For $\mathbf{L_1}$–$\mathbf{L_4}$ see Chart 1.

[b] Unless otherwise noted, the quantum yield of product formation is defined as the formation rate divided by the light intensity.

[c] Unless otherwise noted, TON is defined as the mole of product(s) divided by the mole of catalyst used and TOF is defined as the TON divided by the irradiation time in hours.

[d] With 15% water in DMF.

[e] With 15% water and 10 equiv. bpy in DMF.

[f] Assuming two (or eight) photons produce one molecule of the product.

[g] With 23 equiv. NEt_4Cl added.

[h] In high-pressure CO_2 gas (T = 26 °C, P = 1–2 MPa)/liquid DMF solution.

[i] With 13 equiv. NEt_4Br added.

[j] In liquid CO_2 solution (T = 28 °C, P = 7.0 MPa).

loss results in the stable 18e$^-$ ligand-centered radical species, *fac*-Re(dmb$^{\bullet-}$)(CO)$_3$(solv), which can also be produced by photocleavage of the Re–Re bond in $[Re(dmb)(CO)_3]_2$. This species reacts with CO_2 to form a μ_2–η^2–CO_2 bridged binuclear complex, *fac*, *fac*-(CO)$_3$(dmb)Re–^{13}C(O)O–Re(dmb)(CO)$_3$ as observed by ^{1}H and ^{13}C NMR upon photolysis of a $^{13}CO_2$-saturated DMF-d_7 solution (Fig. 2) [51]. This intermediate was shown to decay with a first-order dependence on $[CO_2]$ to produce CO and CO_3^{2-} and to be accelerated by visible light irradiation [51]. Coordination of the CO_2 reduction by-product CO_3^{2-} to the rhenium center is likely to be the primary source of catalyst deactivation as the Re–OC(O)O–Re species is highly insoluble in the organic solvents typically employed for photocatalysis. In the case of *fac*-Re(NCS)(bpy)(CO)$_3$, Ishitani has proposed that the corresponding OER complex serves as both an electron donor and CO_2 reduction catalyst [7]. Loss of NCS$^-$ from the OER species is followed by coordination of CO_2, and subsequent electron transfer from another OER complex generates CO and, after re-coordination of NCS$^-$, two equivalents of *fac*-Re(NCS)(bpy)(CO)$_3$ with no indication as to the fate of the oxide (Fig. 3) [7]. However, there is no clear evidence

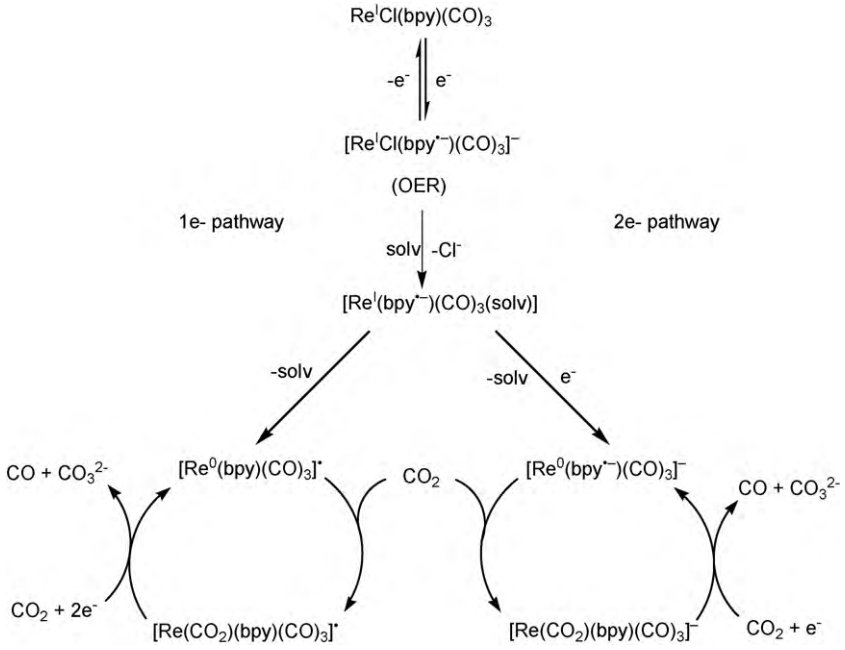

Fig. 1. Proposed one- and two-electron pathways for electrochemical CO_2 reduction [47,48].

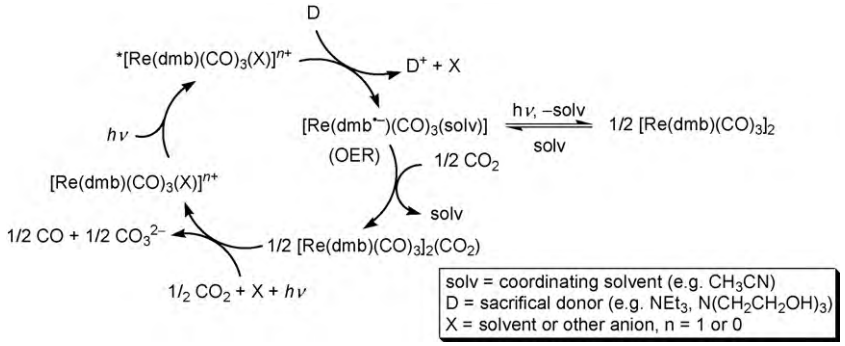

Fig. 2. Mechanism proposed for photochemical CO_2 reduction with $[Re(dmb)(CO)_3]_2$ [51].

for formation of the CO_2 adducts or reduction of CO_2 by an outer-sphere electron-transfer mechanism.

Despite the successful coupling of light absorption to the multielectron catalytic reduction of CO_2, significant challenges remain if these systems are to be used on a global scale for the production of clean fuels and/or fine chemicals by artificial photosynthetic processes. A major hindrance for these catalysts is their poor visible light absorption, with the majority of reported bipyridyl rhenium(I) tricarbonyl complexes possessing MLCT absorption bands in the near-UV ($300\,nm < \lambda_{max} < 400\,nm$) [43]. As is the case for electrocatalysis, chloride loss from the photochemically generated OER species is slow ($k_{obs} < 100\,s^{-1}$ for [*fac*-ReCl(dmb)(CO)$_3$]$^-$ in CH_3CN) [51]. Experimental and theoretical studies indicate that in polar organic solvents (CH_3CN, DMF, THF, etc.) the solvent-coordinated ligand-centered radical is stable, and substitution of bound solvent by CO_2 is extremely slow with an observed rate of $\sim 3 \times 10^{-3}\,s^{-1}$ under 0.8 atm CO_2 (0.22 M) [51,52]. The turnover-limiting step in the photochemical reduction cycle depicted in Fig. 2 is actually the reaction of the μ_2–η^2–CO_2 bridged binuclear species with CO_2 with a bimolecular rate constant of $k = 9.7 \times 10^{-4}\,M^{-1}\,s^{-1}$

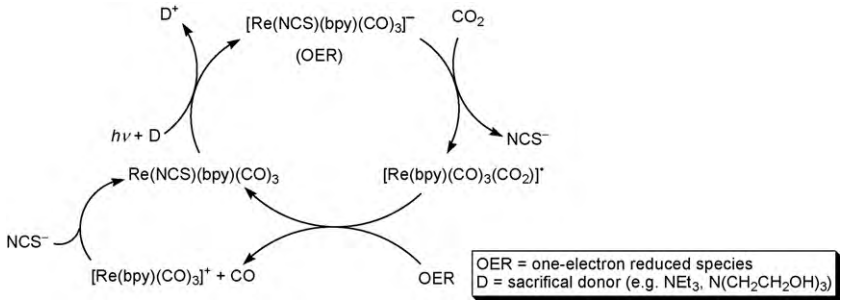

Fig. 3. Mechanism proposed for photochemical CO_2 reduction with *fac*-Re(NCS)(bpy)(CO)$_3$ [7].

Table 3
Photophysical, electrochemical and photochemical properties of some *fac*-ReX(α-diimine)$(CO)_3^{0/+}$ complexes.

α-Diimine	X	Solvent	ν_{CO} (cm^{-1})	λ_{MLCT}, nm ($\varepsilon/10^3$, $M^{-1}\,cm^{-1}$)	λ_{em}, nm (τ_0, ns)	$E_{1/2}$, V	Reductive quenching		Ref.
							k_q ($M^{-1}\,s^{-1}$)	K_{SV} (M^{-1})	
bpy	Cl	CH_3CN	2023, 1917, 1899	370 (3.42)	622 (25)	1.36[a,b], −1.32[a]	2.6×10^{7}[c]	0.71	[45,58]
bpy	Br	THF	2019, 1919, 1895	375[d]	610[d] (55)[d]	−1.91[e], −2.33[e]	6.0×10^{7}[f,g]	3.3	[30,59]
dmb	Cl	CH_3CN	2023, 1906, 1893	360 (3.40)	602 (27)	1.35[h], −1.43[h], −1.98[h]			[50,58,60]
dnb-F_{26}	Cl	CH_3CN	2022, 1916, 1897	368 (4.10)	625 (30)	1.35[a,b], −1.40[a]	2.5×10^{7}[c]	0.76	[45]
dnb-F_{26}	Cl	$scCO_2$[i]	2028, 1933, 1909	394	610[j] (34)		4.4×10^{6}[c]	0.15	[45]
dub-F_{34}	Cl	CH_3CN	2022, 1916, 1898	368 (3.79)	625 (30)	1.35[a,b], −1.39[a]	2.5×10^{7}[c]	0.76	[45]
dub-F_{34}	Cl	$scCO_2$[i]	2028, 1933, 1909	394	610[j] (33)		4.2×10^{6}[c]	0.14	[45]
bpy	$P(OEt)_3$	CH_3CN	2047, 1962, 1927	317 (13.5), 351 sh (3.06)	522 (1034)	1.7[b,k], −1.43[k], −1.87[k,l]	1.1×10^{9}[d,g]	1140	[34,46]
bpy	$P(O^iPr)_3$	CH_3CN	2045, 1958, 1924	315 (14.3), 346 sh (3.37)	521 (952)	1.7[b,k], −1.44[k], −1.89[k,l]	8.6×10^{8}[d,g]	820	[34,46]
bpy	$P(Ohex)_3$	CH_2Cl_2		316 (13.5), 347 (4.6)					[35]
bpy	$P(Ohex)_3$	CO_2, liq[m]		314 (13.9), 340 sh (6.7)	520 (395)				[35]
bpy	NCS	CH_3CN	2027, 1919 br	396 (2.9)[n]	635[d] (30)[d]	−1.61[k]	3.7×10^{8}[d,g]	11	[7]
bpy	CH_3CN	CH_2Cl_2	2032, 1942 br	343 (4.25)	536 (1200)	−1.58[e,o], −1.80[e,o]			[47,57]

[a] vs. SCE.
[b] E_{pa}.
[c] TEA.
[d] recorded in DMF.
[e] vs. Fc/Fc^+.
[f] recorded in CH_3CN.
[g] TEOA.
[h] vs. SSCE.
[i] 35 °C, 13.8 MPa.
[j] uncorrected.
[k] vs. $Ag/AgNO_3$.
[l] E_{pc}.
[m] 26 °C, 7.9 MPa.
[n] recorded in CH_2Cl_2.
[o] recorded in THF:CH_3CN = 3:2 (v/v).

for [*fac*-Re(dmb)$(CO)_3$]$_2(CO_2)$ in DMF, although the reaction can be accelerated more than 50 times under irradiation [51]. These unfavorable kinetic barriers are further exacerbated by the low solubility of CO_2 in conventional organic solvents with [CO_2] of 0.2–0.3 M/atm under ambient conditions [53].

In an effort to increase [CO_2] while simultaneously decreasing or eliminating the ability of coordinating organic solvents to stabilize the 17e$^-$ metal-centered radical, *fac*-Re$^\bullet$(α-diimine)$(CO)_3$, Hori has explored supplementing or replacing organic solvents with high-pressure compressed CO_2 [29,35,36]. Employing liquid CO_2 ($liqCO_2$) or supercritical CO_2 ($scCO_2$) as both reactant and solvent has several benefits. In addition to the elimination of coordinating organic solvents, the physical properties (density, viscosity, etc.) of the CO_2 solvent are tunable as a function of temperature and pressure, while the [CO_2] can be increased to ca. 22 M at 35 MPa (cf., 0.2 M in DMF under ambient conditions) [53,54]. Irradiation of a 2.6×10^{-4} M *fac*-ReCl(bpy)$(CO)_3$ solution in DMF containing 0.8 M TEA with 365 nm monochromatic light under 2.45 MPa of CO_2 resulted in significantly more CO (TON = 41.8 after 25 h) relative to similar photolysis under 0.10 MPa of CO_2 (TON = 8.2 after 25 h) [29]. Increasing the CO_2 pressure further to 7.30 MPa results in a reaction mixture which is one phase, consisting of a homogeneous solution of TEA and DMF in liquid CO_2. However, photolysis of [*fac*-Re(bpy)$(CO)_3${P(O^iPr)$_3$}]$^+$ in this $liqCO_2$/DMF solution with 365 nm light resulted in very low catalytic activity (TON = 0.4 after 16 h) [36]. Elimination of coordinating organic solvents was achieved by preparation of liquid CO_2-soluble cationic rhenium(I) catalysts employing a fluorinated tetra-aryl borate counteranion such as [*fac*-Re(bpy)$(CO)_3${P(Ohex)$_3$}][B(3,5-$(CF_3)_2$-$C_6H_3)_4$] [35]. This catalyst is marginally more active in $liqCO_2$ as compared to conventional solvent, yielding 2.2 turnovers after 2 h under 365 nm irradiation in liquid CO_2 containing 4.4×10^{-5} M catalyst and 0.42 M TEA (T = 28 °C, p = 7.0 MPa, ρ = 0.70 g cm^{-3}) [35]. While incorporating a fluorinated counteranion resulted in increased catalyst solubility in liquid CO_2 solution and increased CO_2 reduction activity (*vide supra*), this approach is not suitable for extension to the neutral *fac*-ReCl(α-diimine)$(CO)_3$ complexes. Furthermore, the low catalytic activity observed in liquid CO_2 (relative to organic solvents) may be due to precipitation of the neutral photogenerated reduced species, *fac*-Re(bpy)$(CO)_3${P(Ohex)$_3$}.

In order to address some of these concerns we have synthesized and characterized neutral CO_2-soluble rhenium bipyridine complexes bearing fluorinated alkyl substituents, which are well-known to impart enhanced solubility to otherwise insoluble metal complexes in $scCO_2$ [54]. Fluorinated bipyridine ligands 4,4′-$(C_6F_{13}CH_2CH_2CH_2)_2$-2,2′-bipyridine (**dnb-$F_{26}$**) and 4,4′-$(C_8F_{17}CH_2CH_2CH_2)_2$-2,2′-bipyridine (**dub-$F_{34}$**) were prepared as reported [55,56] and metalated with $ReCl(CO)_5$ in refluxing

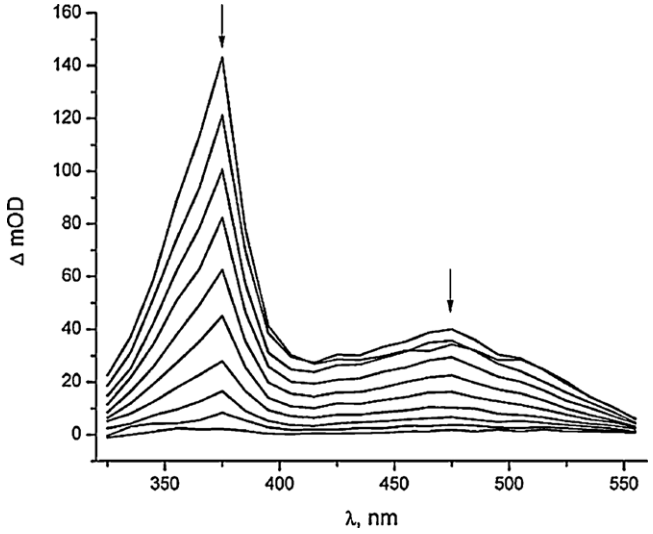

Fig. 4. Transient UV–vis spectra obtained between 8 and 140 ns after 410 nm pulsed laser excitation of a CH_3CN solution of *fac*-ReCl(**dnb-F$_{26}$**)$(CO)_3$ at 25 °C This figure was reproduced from Ref. [45] with permission of the copyright holders.

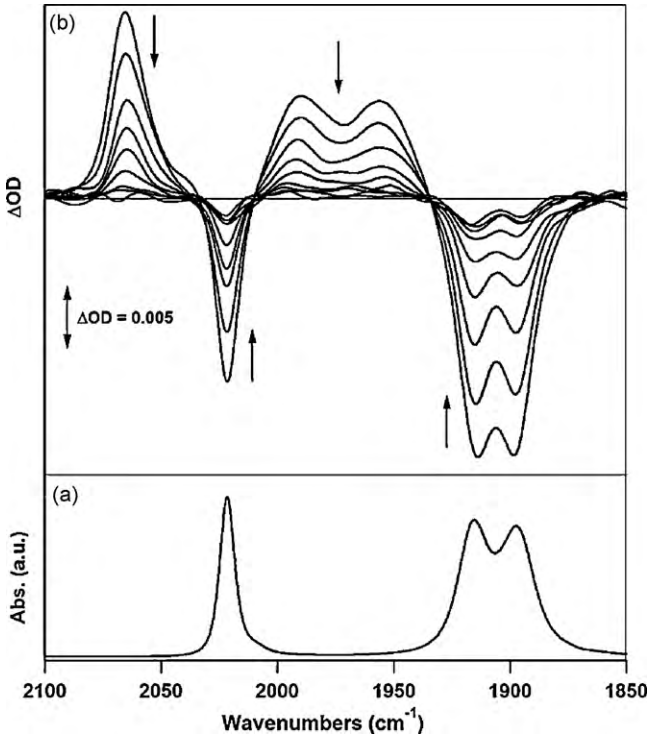

Fig. 5. (a) Fourier transform IR (FTIR) spectrum of *fac*-ReCl(**dnb-F$_{26}$**)$(CO)_3$ in CH_3CN (vs. CH_3CN background at 25 °C). (b) Time-resolved step-scan FTIR spectra recorded between 0 and 115 ns after 410 nm pulsed laser excitation of this solution. Positive bands represent the excited state species, while negative bands represent the ground-state bleach. This figure was reproduced from Ref. [45] with permission of the copyright holders.

toluene to give the corresponding *fac*-ReCl(**dnb-F$_{26}$**)$(CO)_3$ and *fac*-ReCl(**dub-F$_{34}$**)$(CO)_3$ complexes in good yield [45]. The photophysical and electrochemical properties of these complexes are virtually identical to the corresponding *fac*-ReCl(bpy)$(CO)_3$ as a result of the incorporation of three methylene units separating the fluorinated alkyl chains from the bipyridine π system which effectively insulate the metal center from the electron withdrawing properties of the F atoms. This effect is most obvious when comparing the ν_{CO} IR stretching frequencies and reduction potentials of *fac*-ReCl(**dnb-F$_{26}$**)$(CO)_3$ and *fac*-ReCl(**dub-F$_{34}$**)$(CO)_3$ with the analogous unsubstituted complex, *fac*-ReCl(bpy)$(CO)_3$ in CH_3CN (see Table 3). In addition, the excited state properties of these fluorinated bipyridyl complexes are analogous to those reported for the unsubstituted bpy complex with $\lambda_{em} = 625$ nm and $\tau_{em} = 30$ ns in CH_3CN (cf., $\lambda_{em} = 625$ nm and $\tau_{em} = 27$ ns for *fac*-ReCl(bpy)$(CO)_3$) [45]. A hypsochromic shift of the emission band to $\lambda_{em} = 610$ nm and an increase in excited state lifetime ($\tau_{em} = 33$–34 ns) is observed in $scCO_2$ solutions ($T = 35$ °C, $p = 13.8$ MPa) of these complexes as a result of the lower solvent polarity (relative to CH_3CN) which serves to raise the energy of the excited state, consistent with the energy gap law [45,57].

UV–vis transient absorption and time-resolved infrared (TRIR) spectroscopies of *fac*-ReCl(**dnb-F$_{26}$**)$(CO)_3$ or *fac*-ReCl(**dub-F$_{34}$**)$(CO)_3$ in CH_3CN and $scCO_2$ solution are consistent with the formation of a ^{3}MLCT excited state (see Figs. 4 and 5 for transient UV–vis and TRIR spectra of *fac*-ReCl(**dnb-F$_{26}$**)$(CO)_3$ in CH_3CN) [45,58]. Stern-Volmer reductive quenching of the ^{3}MLCT excited state emission of these complexes by TEA occurs rapidly in CH_3CN with quenching rate constants, $k_q \approx 2.5 \times 10^7\ M^{-1}\ s^{-1}$ (cf., $k_q = 2.6 \times 10^7\ M^{-1}\ s^{-1}$ for *fac*-ReCl(bpy)$(CO)_3$; see Table 3 and Fig. 6). In $scCO_2$ solution, reductive quenching is slower than in CH_3CN as a result of the lower polarity of $scCO_2$ ($k_q \approx 4.3 \times 10^6\ M^{-1}\ s^{-1}$), although only by a factor of approximately six [45]. Preliminary photocatalysis experiments in CO_2-saturated DMF and in $scCO_2$ solution using conditions similar to those employed previously in DMF/TEOA mixtures [27,28] show catalytic formation of CO in both solvents while control experiments in the absence of CO_2 show no CO formation. We are currently investigating the photocatalytic activity of these catalysts in $scCO_2$ in order to obtain the optimized TON and TOF for CO_2 reduction.

3. Photogeneration of bio-inspired renewable hydride donors

Natural photosystems in plants convert CO_2 to carbohydrates and O_2 using absorbed photons as energy and water as a reducing agent. The light energy is converted to chemical energy in the form of adenosine triphosphate (ATP) and reduced nicotinamide adenine dinucleotide (phosphate), NAD(P)H, in complicated processes in which a reduced hydrogen equivalent (*i.e.*, hydride) is stored by

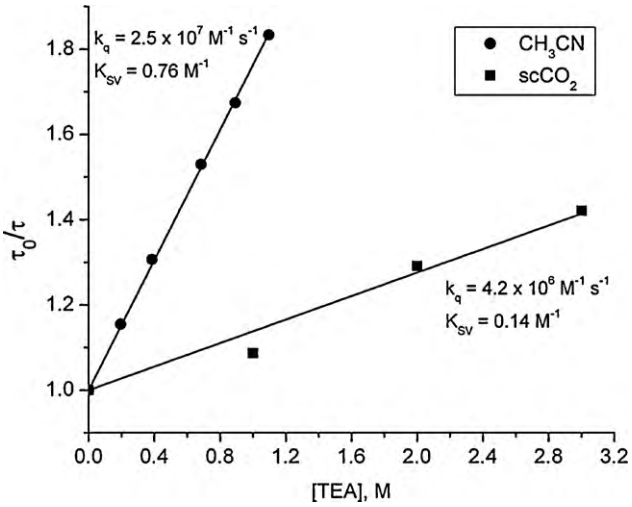

Fig. 6. Stern-Volmer quenching of the emission from the MLCT excited state of *fac*-ReCl(**dnb-F$_{34}$**)$(CO)_3$ by TEA in CH_3CN ($T = 25$ °C) and $scCO_2$ ($T = 35$ °C, $p = 13.8$ MPa). $\lambda_{ex} = 410$ nm. This figure was reproduced from Ref. [45] with permission of the copyright holders.

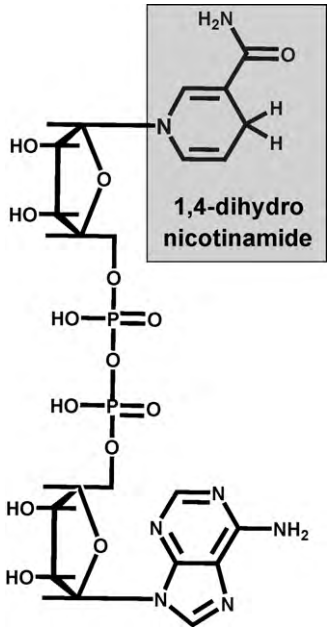

Fig. 7. Structure of NADPH.

the reduction of $NADP^+$. The ATP and NADPH are used to reduce CO_2 in light-independent processes through net hydride-ion transfer reactions. The ability to transfer multiple redox equivalents in the form of H^- (*i.e.*, two electrons and a proton) allows the operation of proton-coupled electron-transfer reactions to avoid high-energy pathways associated with single electron-transfer steps.

Despite the complex structure of NADPH, only a relatively simple fragment, 1,4-dihydronicotinamide acts as the hydride-ion donor (Fig. 7). The chemistry of NADH-model compounds such as 1-benzyl-1,4-dihydronicotinamide (BNAH) or 10-methylacridan, in the reduction of alkyl halides, olefins, ketones, and photoinduced electron transfer, has been extensively studied [61]. However, most of the reactions known to date involving NADH-model complexes are stoichiometric, since the donor regeneration is often highly endoergic and also limited by dimerization via C–C bond formation of the radical species $NAD^•$, which is an intermediate in hydride formation or transfer reactions. The use of hydride donors in multielectron proton-coupled processes, such as CO_2 reduction, would be extremely attractive if the hydride donors could be efficiently regenerated.

One of the very promising photochemical approaches to homogeneous carbon dioxide reduction is a succession of hydride-ion and proton-transfer reactions as illustrated in Scheme 1 for CO_2 that is C-bonded to transition-metal catalytic centers. Specific implementations of these reaction schemes are a good foundation for kinetically efficient CO_2 reduction using transition-metal complexes as catalysts and photocatalysts. In order to implement this path, hydride donors should be cleanly generated photochemically, avoiding the coupling of carbon centered radical intermediates, which can lead to catalyst deactivation. The use of NADH-like moities as ligands of transition metals enables the utilization of MLCT transitions and provides a convenient strategy for light induced hydride generation. However, this approach presents some challenges, in particular those related to the fact that each photon absorbed results in the formation of only the OER species, while hydride donors are two-electron reduced compounds. Therefore, formation of hydride donors will involve complicated multiple-redox reactions to produce the final product.

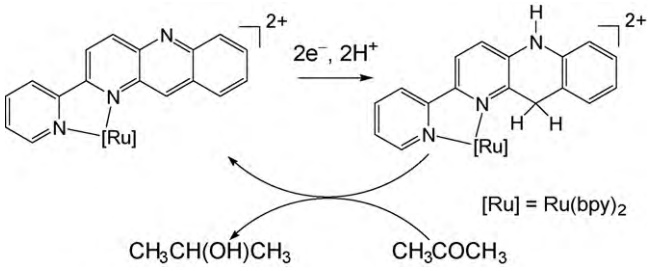

Fig. 8. Catalytic cycle for electrochemical reduction of acetone with $[Ru(bpy)_2(pbnHH)]^{2+}$.

One of the transition-metal complexes containing a NADH-like ligand, $[Ru(bpy)_2(pbn)]^{2+}$ (pbn = 2-(2-pyridyl)-benzo[*b*]-1,5-naphthyridine), was reported to catalytically reduce acetone to isopropanol under electrochemical conditions (−1.14 V vs. Fc/Fc^+) in an acidic medium. This was the first example of electrochemical *catalytic* reduction of organic molecules by NAD(P)H model complexes [62]. $[Ru(bpy)_2(pbnHH)]^{2+}$ (pbnHH = 5,10-dihydro-2-(2-pyridyl)-benzo[*b*]-1,5-naphthyridine) was proposed as the key intermediate as shown in Fig. 8. The reduced species $[Ru(bpy)_2(pbnHH)]^{2+}$ was synthesized chemically using $Na_2S_2O_4$ and characterized by spectroscopy and its single-crystal X-ray diffraction structure [63].

These results have prompted more extensive studies of mechanistic details for the formation of $[Ru(bpy)_2(pbnHH)]^{2+}$ [63,64]. It was demonstrated that the presence of the pbn ligand gives rise to a new absorption band arising from a MLCT transition (d_{Ru}–$\pi_{pbn}{}^*$), and excitation into this band leads to a charge transfer from the metal center mainly to the pbn ligand. The quenching of the excited state of $[Ru(bpy)_2(pbn)]^{2+}$ is readily achieved with sacrificial electron donors with high rates, e.g., $1.1 \times 10^9\ M^{-1}\ s^{-1}$ for DABCO (1,4-diazabicyclo[2.2.2]octane), yielding the OER species, $[Ru(bpy)_2(pbn^{•-})]^+$. The bulk photolysis of an acetonitrile solution of $[Ru(bpy)_2(pbn)]^{2+}$ under 355 nm irradiation in the presence of triethylamine as a sacrificial electron donor exclusively yields $[Ru(bpy)_2(pbnHH)]^{2+}$ with a quantum yield of 21%. This experiment demonstrated that renewable $[Ru(bpy)_2(pbnHH)]^{2+}$ can be cleanly generated photochemically in high quantum yield avoiding formation of side products related to the ruthenium complex.

The mechanism of the formation of $[Ru(bpy)_2(pbnHH)]^{2+}$ was studied using radiation chemistry techniques, since these provide a convenient and clean way to generate OER species. The one-electron reduction of $[Ru(bpy)_2(pbn)]^{2+}$ in buffered aqueous solutions was readily achieved in reactions with the solvated electron (e_{aq}^-, −2.90 V vs. NHE) or the formate radical ($CO_2^{•-}$, −1.90 V vs. NHE), both strong reducing agents. Both e_{aq}^- and $CO_2^{•-}$ were produced using an electron accelerator for transient measurements or a ^{60}Co γ-ray source for bulk radiolysis experiments. The reduction of $[Ru(bpy)_2(pbn)]^{2+}$ with e_{aq}^- or $CO_2^{•-}$ results in the formation of the OER species $[Ru(bpy)_2(pbn^{•-})]^+$ with bimolecular rates $k_1 = 3.0 \times 10^{10}$ and $k_2 = 4.6 \times 10^9\ M^{-1}\ s^{-1}$, respectively (Eqs.

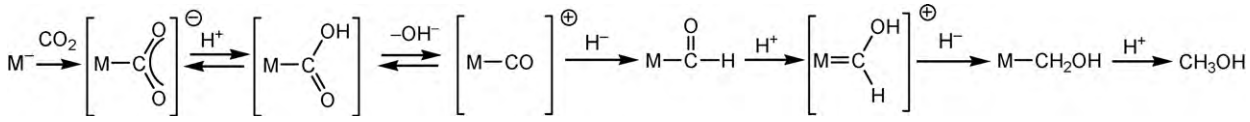

Scheme 1. Reduction of CO_2 by hydride transfer reactions.

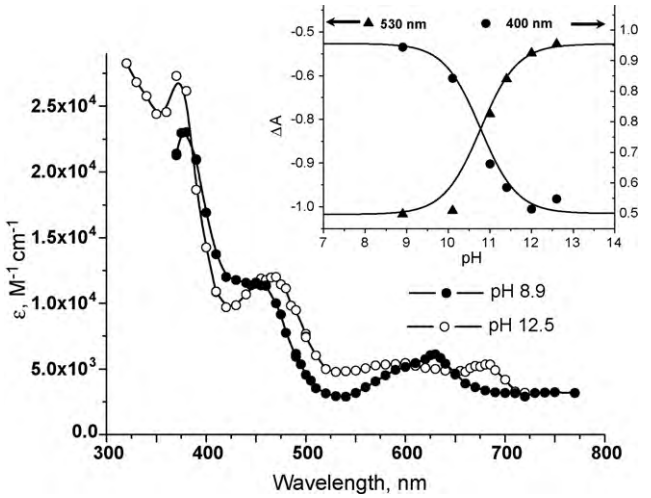

Fig. 9. Spectra of $[Ru(bpy)_2(pbn^{\bullet-})]^+$ (open circles) and $[Ru(bpy)_2(pbnH^{\bullet})]^{2+}$ (solid circles) measured in pulse radiolysis (PR) experiments at pH 12.5 and 8.9, respectively. Insert: pK_a of $[Ru(bpy)_2(pbnH^{\bullet})]^{2+}$ determined by spectroscopic titration of the OER species produced in PR experiments [64].

(1) and (2)), analogous to the photochemical experiments in which the reaction between the excited state $[^*Ru(bpy)_2(pbn)]^{2+}$ and a sacrificial electron donor D also yields the OER species (Eq. (3)):

$$[Ru(bpy)_2(pbn)]^{2+} + e_{aq}^- \rightarrow [Ru(bpy)_2(pbn^{\bullet-})]^+ \quad (1)$$

$$[Ru(bpy)_2(pbn)]^{2+} + CO_2^{\bullet-} \rightarrow [Ru(bpy)_2(pbn^{\bullet-})]^+ + CO_2 \quad (2)$$

$$[*Ru(bpy)_2(pbn)]^{2+} + D \rightarrow [Ru(bpy)_2(pbn^{\bullet-})]^+ + D^{\bullet+} \quad (3)$$

The OER species $[Ru(bpy)_2(pbn^{\bullet-})]^+$ can also be produced by reduction of the parent compound with sodium amalgam, and its UV–vis spectrum matches well the spectra of the OER species produced in pulse radiolysis and photochemical experiments. This indicates that the first step in the production of $[Ru(bpy)_2(pbnHH)]^{2+}$ is the formation of the OER species and is the same for both photo- or radiation-initiated reactions. In support of the above conclusion, the continuous radiolysis of $[Ru(bpy)_2(pbn)]^{2+}$ in buffered aqueous solutions cleanly produces $[Ru(bpy)_2(pbnHH)]^{2+}$. In aqueous solution, the OER species exists in equilibrium with its conjugate acid with $pK_a = 11$ (Eq. (4)), as determined by measuring pH-dependent spectra after one-electron reduction of $[Ru(bpy)_2(pbn)]^{2+}$ in pulse radiolysis experiments (Fig. 9):

$$[Ru(bpy)_2(pbn^{\bullet-})]^+ + H^+ \leftrightarrow [Ru(bpy)_2(pbnH^{\bullet})]^{2+} \quad (4)$$

These results agree well with the pH-dependent electrochemical reduction of $[Ru(bpy)_2(pbn)]^{2+}$, which clearly demonstrates the pK_a of the OER species at ca. 11 (Fig. 10). The OER protonated and non-protonated species are transient in nature, and decay through multiple pathways to yield the final product $[Ru(bpy)_2(pbnHH)]^{2+}$. The observed kinetics for disappearance of the OER species follows a bimolecular rate law as determined in pulse radiolysis experiments, and depends on the pH of the solution. These types of pH-dependent redox reactions are typically analyzed with, e.g., Eq. (9) [65]. The following reactions describe the disappearance of the OER species:

$$[Ru(bpy)_2(pbnH^{\bullet})]^{2+} \overset{K_a}{\rightleftharpoons} [Ru(bpy)_2(pbn^{\bullet-})]^+ + H^+ \quad (5)$$

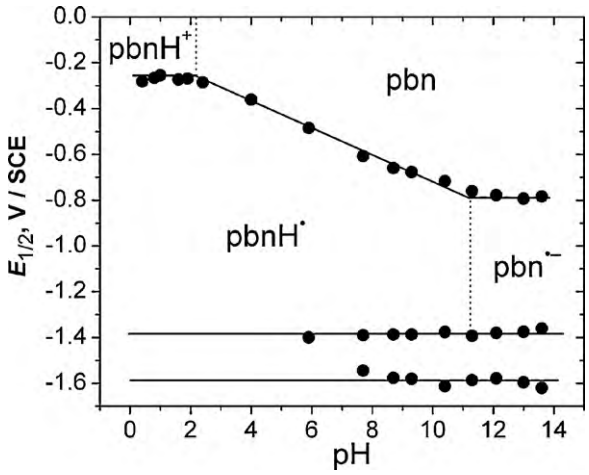

Fig. 10. Pourbaix diagram representing pH-dependent electrochemical reduction of $[Ru(bpy)_2(pbn)]^{2+}$ in aqueous buffer solutions (10% acetonitrile). The two lines below −1.4 V indicate the reduction of bpy. This figure was reproduced from Ref. [63], copyright Wiley-VCH Verlag GmbH & Co. KGaA with permission.

$$2[Ru(bpy)_2(pbnH^{\bullet})]^{2+} \rightarrow [Ru(bpy)_2(pbn)]^{2+} + [Ru(bpy)_2(pbnHH)]^{2+} \quad (6)$$

$$[Ru(bpy)_2(pbnH^{\bullet})]^{2+} + [Ru(bpy)_2(pbn^{\bullet-})]^+ + HA \rightarrow [Ru(bpy)_2(pbn)]^{2+} + [Ru(bpy)_2(pbnHH)]^{2+} + A^- \quad (7)$$

$$2[Ru(bpy)_2(pbn^{\bullet-})]^+ + 2HA \rightarrow [Ru(bpy)_2(pbn)]^{2+} + [Ru(bpy)_2(pbnHH)]^{2+} + 2A^- \quad (8)$$

The observed rate of disappearance of the OER species can be described as follows:

$$k_{obs} = \frac{2\left[k_6 + k_7 K_a/[H^+] + k_8 (K_a/[H^+])^2\right]}{\left(1 + K_a/[H^+]\right)^2} \quad (9)$$

This proposed model agrees well with the experimental kinetic data (Fig. 11) indicating that both disproportionation (Eq. (6))

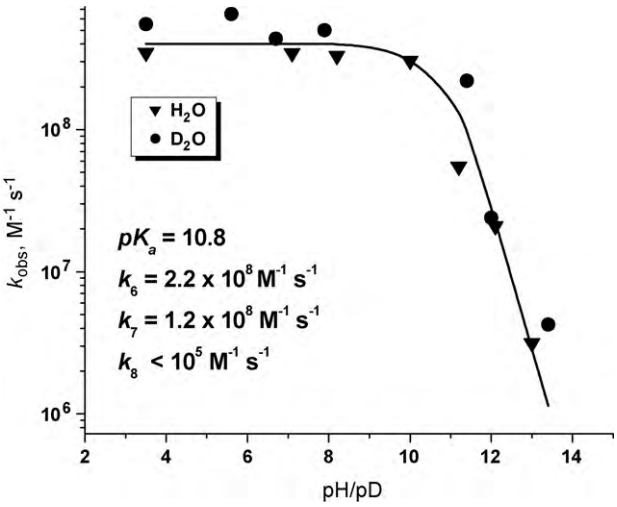

Fig. 11. The dependence of the observed second-order rate constant for disappearance of the OER species on pH (in H_2O triangles; in D_2O dots) and the fit with Eq. (9) [64].

and the cross-reaction (Eq. (7)) are efficient, while the reaction between two non-protonated reduced species is slow (Eq. (8)). This last observation is not surprising since the formation of the two-electron-reduced species is thermodynamically highly unfavorable. The lack of an observable kinetic isotope effect for disproportionation of the OER species indicates that a proton-coupled electron transfer or hydrogen atom transfer is not involved in the rate-determining step.

A detailed analysis of the spectroscopic data measured in pulse radiolysis experiments revealed that while the cross-reaction between the OER protonated and non-protonated species (Eq. (7)) yields the final product and starting material directly, the disproportionation reaction (Eq. (6)) proceeds through the formation of an intermediate. This intermediate was isolated as a product of bulk radiolysis of $[Ru(bpy)_2(pbn)]^{2+}$ at low temperature (0.2 °C), and its UV–vis spectrum matched well the spectrum of the transient species measured after disappearance of OER species produced in pulse radiolysis experiments (Fig. 12). Warming the solution containing the intermediate species to room temperature resulted in a UV–vis spectrum consistent with a 1:1 mixture of $[Ru(bpy)_2(pbn)]^{2+}$ and $[Ru(bpy)_2(pbnHH)]^{2+}$. Based on these results, it was concluded that the intermediate species is dinuclear in nature and can possibly be described as the π-stacked dimer of two $[Ru(bpy)_2(pbnH^{\bullet})]^{2+}$ species. This assumption is supported by the results of the analysis of spin densities in the SOMOs of $[Ru(bpy)_2(pbnH^{\bullet})]^{2+}$ and its conjugate base, $[Ru(bpy)_2(pbn^{\bullet-})]^{+}$, as determined by DFT calculations, which show a substantial localization of the electron density of the unpaired electron on the carbon atom of the naphthyridine ligand (para position from the nitrogen in the central ring of naphthyridine) in the protonated, but not in the non-protonated OER species. The increase of electron density on the naphthyridine moiety may facilitate interaction between the π-systems of two $[Ru(bpy)_2(pbn^{\bullet-})]^{+}$ species. DFT calculations on the π-stacking dimer in a polarizable continuum model for acetonitrile as solvent revealed a structure supporting the proposed disproportionation intermediate. They also helped to identify the intermediate in the cross-reaction between $[Ru(bpy)_2(pbnH^{\bullet})]^{2+}$ and $[Ru(bpy)_2(pbn^{\bullet-})]^{+}$ as being a hydrogen-bonded dimer. As a result of all experimental observations mentioned above, the proposed mechanism for the formation of $[Ru(bpy)_2(pbnHH)]^{2+}$ is shown in Fig. 13.

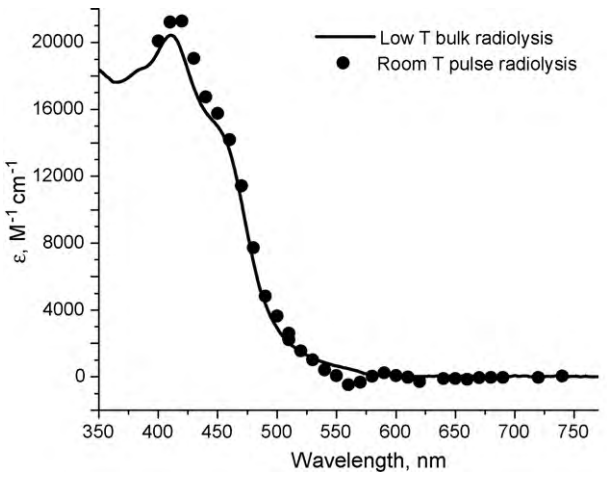

Fig. 12. The spectrum of the $[Ru(bpy)_2(pbnH^{\bullet})]_2^{4+}$ species observed in room-temperature pulse radiolysis (dots) and low-temperature (0.2 °C) bulk radiolysis (line) experiments. This figure was reproduced from Ref. [64] with permission of the copyright holders.

Preliminary DFT calculations on the hydricities of $[Ru(bpy)_2(pbnHH)]^{2+}$ and other potential hydride donors and acceptors relevant to CO_2 reduction have been carried out. Significant among the findings from this work was the prediction of a stronger hydride donor, $[Ru(bpy)_2(pbnHH)]^{+}$, possibly produced upon further visible excitation of $[Ru(bpy)_2(pbnHH)]^{2+}$ followed by reductive quenching, and the prediction that this further-reduced species is capable of donating a hydride ion to a carbonyl ligand of a second (acceptor) transition-metal complex. Preliminary experiments have confirmed that $[Ru(bpy)_2(pbnHH)]^{2+}$ can donate a hydride ion to the trityl cation, and experiments using

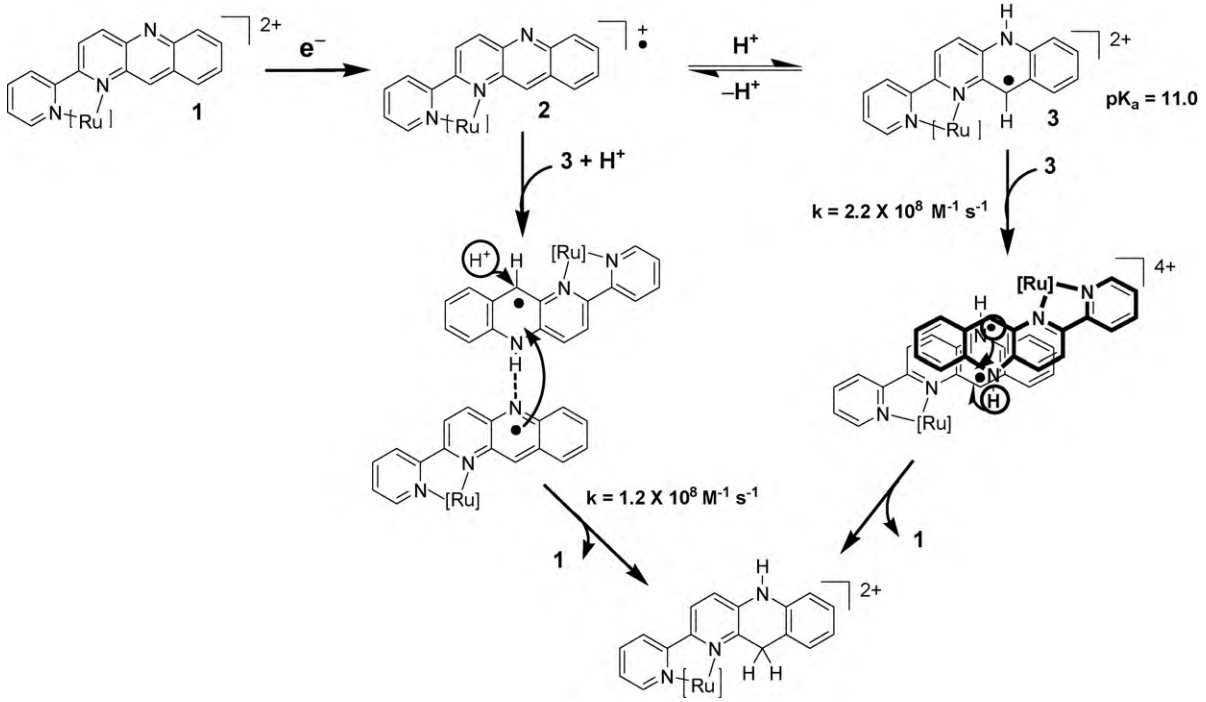

Fig. 13. The proposed mechanism of formation of $[Ru(bpy)_2(pbnHH)]^{2+}$ in aqueous medium.

$[Ru(bpy)_2(pbnHH)]^+$ are underway to explore the prediction of M–CHO formation from $[M–CO]^+$ by hydride ion transfer.

In summary, synthetic systems based on the NADH-like functionality coupled to a light absorbing chromophore offer an attractive approach to achieve photocatalytic reduction of carbon dioxide driven by absorption of visible light. The ability of hydride donors to transfer multiple proton-coupled redox equivalents in the form of the hydride ion allows the avoidance of high-energy intermediates usually associated with one-electron or one-proton processes. This makes hydride donors potential reagents of choice for the efficient catalytic reduction of CO_2. However, many challenges remain in achieving successful and efficient hydride transfer reactions to M–CO species using renewable hydrides produced by light absorption.

The ruthenium complex $[Ru(bpy)_2(pbn)]^{2+}$ is the first example of a photochemically generated reversible hydride donor that is reported to catalyze the electrochemical reduction of the carbonyl group of a model compound, acetone, in acidic conditions. The excited state of $[Ru(bpy)_2(pbn)]^{2+}$ is readily quenched to produce the OER species that can cleanly disproportionate to yield the final $[Ru(bpy)_2(pbnHH)]^{2+}$ product. This disproportionation reaction allows the pooling of the energy of two photons to generate a two-electron-reduced hydride donor molecule. The localization of electron density of the unpaired electron on the part of the naphthyridine ligand surrounded by a bulky environment prevents the dimerization of the OER species, thus making the generation of the hydride donor clean and efficient.

Understanding the mechanism of hydride transfer from a hydride donor to an acceptor is another crucial step in designing efficient catalysts for photochemical CO_2 reduction. Preliminary investigations indicate that while photogenerated $[Ru(bpy)_2(pbnHH)]^{2+}$ transfers a hydride to the trityl cation to recover the parent $[Ru(bpy)_2(pbn)]^{2+}$, $[Ru(bpy)_2(pbnHH)]^{2+}$ is not a strong enough hydride donor to reduce either free CO_2 or metal complexes with CO or CO_2 ligands. However, our preliminary theoretical predictions indicate that the further-reduced species $[Ru(bpy)_2(pbnHH)]^+$ is a significantly stronger hydride donor that can potentially be used to reduce carbonyl ligands of metal complexes. This appears to open a new door to the stepwise photoreduction of metal carbonyls to methanol. Our ongoing research will be published in a forthcoming paper.

4. Conclusion

This article summarizes recent progress in our laboratories in the areas of photocatalytic reduction of CO_2 and photochemical generation of a renewable hydride donor. The incorporation of fluorinated substituents into the $Re^IX(bipyridyl)(CO)_3$ family of complexes using **dnb-F$_{26}$** and **dub-F$_{34}$** has imparted solubility in $scCO_2$ to these photocatalysts without significantly altering their electronic or photophysical properties. Stern-Volmer reductive quenching of the MLCT excited state emission of these complexes with TEA occurs rapidly in both CH_3CN and $scCO_2$, with quenching rate constants only approximately six times slower in $scCO_2$. Preliminary photochemical experiments suggest that in CO_2-saturated DMF and $scCO_2$ solution containing TEOA or TEA, these complexes catalyze the reduction of CO_2 to CO.

A ruthenium(II) complex bearing a NADH inspired ligand, $[Ru(bpy)_2(pbn)]^{2+}$ has been prepared and upon reductive quenching of the photogenerated MLCT excited state, produces a OER species which ultimately disproportionates to cleanly form $[Ru(bpy)_2(pbnHH)]^{2+}$. This disproportionation allows the energy of two photons to be pooled to generate a two-electron reduced hydride donor, which is capable of transferring a hydride to the trityl cation. Furthermore, preliminary theoretical studies suggest the three-electron reduced species, $[Ru(bpy)_2(pbnHH)]^+$ would be a much stronger hydride donor capable of reducing carbonyl ligands of transition-metal complexes.

Acknowledgements

EF thanks Professor Koji Tanaka and Dr. Takashi Fukushima at the Institute for Molecular Science for discussions. EF and DEP thank Dr. Diane Cabelli (BNL) for her help on radiolysis experiments. The work at Brookhaven National Laboratory is funded under contract DE-AC02-98CH10886 with the U.S. Department of Energy and supported by its Division of Chemical Sciences, Geosciences, & Biosciences, Office of Basic Energy Sciences. The authors also thank the U.S Department of Energy for funding under the BES Solar Energy Utilization initiative.

References

[1] http://co2now.org/.
[2] N.S. Lewis, D.G. Nocera, Proc. Natl. Acad. Sci. U.S.A. 103 (2006) 15729.
[3] Intergovenmental Panel on Climate Change, 2008.
[4] M.M.M. Halman, Steinberg Greenhouse Gas Carbon Dioxide Mitigation: Science and Technology, Lewis Publisher, Boca Raton, 1999.
[5] H.A. Schwarz, R.W. Dodson, J. Phys. Chem. 93 (1989) 409.
[6] E. Fujita, Coord. Chem. Rev. 186 (1999) 373.
[7] H. Takeda, K. Koike, H. Inoue, O. Ishitani, J. Am. Chem. Soc. 130 (2008) 2023.
[8] J.-M. Lehn, R. Ziessel, J. Organomet. Chem. 382 (1990) 157.
[9] N. Kitamura, S. Tazuke, Chem. Lett. (1983) 1109.
[10] J.-M. Lehn, R. Ziessel, Proc. Natl. Acad. Sci. U.S.A. 79 (1982) 701.
[11] R. Ziessel, J. Hawecker, J.M. Lehn, Helv. Chim. Acta 69 (1986) 1065.
[12] H. Ishida, K. Tanaka, T. Tanaka, Organometallics 6 (1987) 181.
[13] H. Ishida, K. Tanaka, T. Tanaka, Chem. Lett. (1988) 339.
[14] H. Ishida, T. Terada, K. Tanaka, T. Tanaka, Inorg. Chem. 29 (1990) 905.
[15] A.H.A. Tinnemans, T.P.M. Koster, D. Thewissen, A. Mackor, Recl. Trav. Chim. Pays-Bas 103 (1984) 288.
[16] C.A. Craig, L.O. Spreer, J.W. Otvos, M. Calvin, J. Phys. Chem. 94 (1990) 7957.
[17] J.L. Grant, K. Goswami, L.O. Spreer, J.W. Otvos, M. Calvin, J. Chem. Soc., Dalton Trans. (1987) 2105.
[18] E. Kimura, X. Bu, M. Shionoya, S. Wada, S. Maruyama, Inorg. Chem. 31 (1992) 4542.
[19] E. Kimura, S. Wada, M. Shionoya, Y. Okazaki, Inorg. Chem. 33 (1994) 770.
[20] R. Maidan, I. Willner, J. Am. Chem. Soc. 108 (1986) 8100.
[21] I. Willner, R. Maidan, D. Mandler, H. Dürr, G. Dörr, K. Zengerle, J. Am. Chem. Soc. 109 (1987) 6080.
[22] S. Matsuoka, K. Yamamoto, T. Ogata, M. Kusaba, N. Nakashima, E. Fujita, S. Yanagida, J. Am. Chem. Soc. 115 (1993) 601.
[23] T. Ogata, S. Yanagida, B.S. Brunschwig, E. Fujita, J. Am. Chem. Soc. 117 (1995) 6708.
[24] T. Ogata, Y. Yamamoto, Y. Wada, K. Murakoshi, M. Kusaba, N. Nakashima, A. Ishida, S. Takamuku, S. Yanagida, J. Phys. Chem. 99 (1995) 11916.
[25] J. Grodkowski, D. Behar, P. Neta, P. Hambright, J. Phys. Chem. A 101 (1997) 248.
[26] D. Behar, T. Dhanasekaran, P. Neta, C.M. Hosten, D. Ejeh, P. Hambright, E. Fujita, J. Phys. Chem. A 102 (1998) 2870.
[27] J. Hawecker, J.-M. Lehn, R. Ziessel, J. Chem. Soc. Chem. Commun. (1983) 536.
[28] J. Hawecker, J.-M. Lehn, R. Ziessel, Helv. Chim. Acta 69 (1986) 1990.
[29] H. Hori, Y. Takano, K. Koike, Y. Sasaki, Inorg. Chem. Commun. 6 (2003) 300.
[30] C. Kutal, M.A. Weber, G. Ferraudi, D. Geiger, Organometallics (1985) 2161.
[31] C. Kutal, A.J. Corbin, G. Ferraudi, Organometallics 6 (1987) 553.
[32] H. Hori, F.P.A. Johnson, K. Koike, K. Takeuchi, Takashi, O. Ibusuki, Ishitani, J. Chem. Soc., Dalton Trans. (1997) 1019.
[33] H. Hori, F.P.A. Johnson, K. Koike, O. Ishitani, T. Ibusuki, J. Photochem. Photobiol. A: Chem. 96 (1996) 171.
[34] K. Koike, H. Hori, M. Ishizuka, J.R. Westwell, K. Takeuchi, T. Ibusuki, K. Enjouji, H. Konno, K. Sakamoto, O. Ishitani, Organometallics 16 (1997) 5724.
[35] H. Hori, K. Koike, K. Takeuchi, Y. Sasaki, Chem. Lett. (2000) 522.
[36] H. Hori, K. Koike, Y. Suzuki, M. Ishizuka, J. Tanaka, K. Takeuchi, Y. Sasaki, J. Mol. Catal. A: Chem. 179 (2002) 1.
[37] H. Hori, J. Ishihara, K. Koike, K. Takeuchi, T. Ibusuki, O. Ishitani, J. Photochem. Photobiol. A: Chem. 120 (1999) 119.
[38] B. Gholamkhass, H. Mametsuka, K. Koike, T. Tanabe, M. Furue, O. Ishitani, Inorg. Chem. 44 (2005) 2326.
[39] S. Sato, K. Koike, H. Inoue, O. Ishitani, Photochem. Photobiol. Sci. 6 (2007) 454.
[40] K. Koike, S. Naito, S. Sato, Y. Tamaki, O. Ishitani, J. Photochem. Photobiol A: Chem. (2009).
[41] Z.-Y. Bian, K. Sumi, M. Furue, S. Sato, K. Koike, O. Ishitani, Inorg. Chem. 47 (2008) 10801.
[42] Z.-Y. Bian, K. Sumi, M. Furue, S. Sato, K. Koike, O. Ishitani, J. Chem. Soc., Dalton Trans. (2009) 983.

[43] E. Fujita, B.S. Brunschwig, in: V. Balzani (Ed.), In Electron Transfer in Chemistry, Wiley, VCH, New York, 2001, p. 88.
[44] D.J. Stufkens, A. Vlcek Jr., Coord. Chem. Rev. 177 (1998) 127.
[45] M.D. Doherty, D.C. Grills, E. Fujita, Inorg. Chem. 48 (2009) 1796.
[46] H. Hori, K. Koike, M. Ishizuka, K. Takeuchi, T. Ibusuki, O. Ishitani, J. Organomet. Chem. 530 (1997) 169.
[47] F.P.A. Johnson, M.W. George, F. Hartl, J.J. Turner, Organometallics 15 (1996) 3374.
[48] B.P. Sullivan, C.M. Bolinger, D. Conrad, W.J. Vining, T.J. Meyer, J. Chem. Soc., Chem. Commun. (1985) 1414.
[49] D.H. Gibson, X. Yin, H. He, M.S. Mashuta, Organometallics 22 (2003) 337.
[50] P. Christensen, A. Hamnett, A.V.G. Muir, J.A. Timney, J. Chem. Soc., Dalton Trans. (1992) 1455.
[51] Y. Hayashi, S. Kita, B.S. Brunschwig, E. Fujita, J. Am. Chem. Soc. 125 (2003) 11976.
[52] E. Fujita, J.T. Muckerman, Inorg. Chem. 43 (2004) 7636.
[53] A. Gennaro, A.A. Isse, E. Vianello, J. Electroanal. Chem. 289 (1990) 203.
[54] P.G. Jessop, T. Ikariya, R. Noyori, Chem. Rev. 99 (1999) 475.
[55] B.L. Bennett, K.A. Robins, R. Tennant, K. Elwell, F. Ferri, I. Bashta, G. Aguinaldo, J. Fluorine Chem. 127 (2006) 140.
[56] J. Xia, T. Johnson, S.G. Gaynor, K. Matyjaszewski, J. DeSimone, Macromolecules 32 (1999) 4802.
[57] J.V. Caspar, T.J. Meyer, J. Phys. Chem. 87 (1983) 952.
[58] K. Kalyanasundaram, J. Chem. Soc., Faraday Trans. 2 (82) (1986) 2401.
[59] G.J. Stor, F. Hartl, J.W.M. van Outersterp, D.J. Stufkens, Organometallics 14 (1995) 1115.
[60] A.I. Breikss, H.D. Abruña, J. Electroanal. Chem. 201 (1986) 347.
[61] For example:
(a) S. Fukuzumi, in: P.S. Mariano (Ed.), Advances in Electron-Transfer Chemistry, JAI Press Inc., Greenwich, CT, 1992, pp. 67–175;
(b) J. Gębicki, A. Marcinek, J. Zielonka, Acc. Chem. Res. 37 (2004) 379;
(c) S. Fukuzumi, O. Inada, T. Suenobu, J. Am. Chem. Soc. 125 (2003) 4808;
(d) X.-Q. Zhu, Y. Yang, M.J. Zhang, -P. Cheng, J. Am. Chem. Soc. 125 (2003) 15298;
(e) I. Nakanishi, K. Ohkubo, S. Fujita, S. Fukuzumi, T. Konishi, M. Fujitsuka, O. Ito, N. Miyata, J. Chem. Soc., Perkin Trans. 2 (2002) 1829;
(f) S. Fukuzumi, H. Imahori, K. Okamoto, H. Yamada, M. Fujitsuka, O. Ito, D.M. Guldi, J. Phys. Chem. A 106 (2002) 1903;
(g) R. Reichenbach-Klinke, M. Kruppa, B. König, J. Am. Chem. Soc. 124 (2002) 12999;
(h) X.-Q. Zhu, H.-R. Li, Q. Li, T. Ai, J.-Y. Lu, Y. Yang, J.-P. Cheng, Chem. Eur. J. 9 (2003) 871;
(i) Y. Lu, Y. Zhao, K.L. Handoo, V.D. Parker, Org. Biomol. Chem. 1 (2003) 173;
(j) U. Gran, Tetrahedron 59 (2003) 4303;
(k) X.-Q. Zhu, L. Cao, Y. Liu, Y. Yang, J.-Y. Lu, J.-S. Wang, J.-P. Cheng, Chem. Eur. J. 9 (2003) 3937;
(l) Y. Mikata, S. Aida, S. Yano, Org. Lett. 6 (2004) 2921;
(m) C. Selvaraju, P. Ramamurthy, Chem. Eur. J. 10 (2004) 2253;
(n) S.C. Ritter, M. Eiblmaier, V. Michlova, B. König, Tetrahedron 61 (2005) 5241;
(o) H. Buck, Int. J. Quant. Chem. 101 (2005) 389;
(p) O. Ishitani, N. Inoue, K. Koije, T. Ibusuki, J. Chem. Soc. Chem. Commun. (1994) 367;
(q) A. Kobayashi, K. Sakamoto, O. Ishitani, Inorg. Chem. Commun. 8 (2005) 365;
(r) M. Tanaka, K. Ohkubo, S. Fukuzumi, J. Am. Chem. Soc. 128 (2006) 12372;
(s) J. Yuasa, S. Yamada, S. Fukuzumi, J. Am. Chem. Soc. 128 (2006) 14938;
(t) M. Ishikawa, S. Fukuzumi, J. Am. Chem. Soc. 112 (1990) 8864;
and references therein.
[62] T. Koizumi, K. Tanaka, Angew. Chem. Int. Ed. (2005) 5891.
[63] D. Polyansky, D. Cabelli, J.T. Muckerman, E. Fujita, T. Koizumi, T. Fukushima, T. Wada, K. Tanaka, Angew. Chem. Int. Ed. 46 (2007) 4169.
[64] D.E. Polyansky, D. Cabelli, J.T. Muckerman, T. Fukushima, K. Tanaka, E. Fujita, Inorg. Chem. 47 (2008) 3958.
[65] F. Casalboni, Q.G. Mulazzani, C.D. Clark, M.Z. Hoffman, P.L. Orizondo, M.W. Perkovic, D.P. Rillema, Inorg. Chem. 36 (1997) 2252.